Petrographic Analysis of HSDP-2 Basalts From Hawaii Scientific Drilling Project: Magma Source Compositions and Olivine Accumulation

Shelley D. Miller {smille11@utk.edu}
Earth and Planetary Sciences, University of Tennessee, Knoxville, TN 37996-1410

ABSTRACT

Phase 2 of the Hawaii Scientific Drilling Project (HSDP-2) collected approximately 3098 m of continuous samples that represent the most complete eruptive history of the Mauna Kea (MK) hot spot volcano. The goal of the HSDP is to use the temporal and geochemical evolution of MK to better understand the spatial geochemical structure of the underlying mantle plume. The purpose of this study is to determine if MK basalts from HSDP-2 define an olivine control line and if the whole-rock compositions represent the liquid from which the lavas crystallized. 35 tholeiitic and alkali basalts from the MK volcano were examined petrographically to quantify olivine phenocrysts abundance. Olivine phenocrysts range in size from 0.4-4.6mm and vary in abundance from 5.3-50.3 vol%. HSDP-2 samples display a wide range of textures; crystals within each sample vary in size, shape, abundance, and degree of alteration. When compared to bulk MgO, olivine phenocrysts define an olivine control line with and R2 value of 0.85. The magma crystallization model MELTS {*Ghiorso et al., 1995*} was used to determine whether the composition of the olivine measured in selected HSDP-2 samples represents the equilibrium olivine expected for a given bulk composition (MgO). HSDP-2 samples with Mg#≥75 and forsterite (Fo) content (measured < modeled) contain accumulated olivine. Thus, not all HSDP-2 lavas are representative of mantle compositions; select samples must be corrected for accumulated olivine. Samples with Mg#<75 whose olivine composition falls below the equilibrium Fo range probably reflect the lack of measuring the most Fo-rich phenocryst. Although the compositional data set for HSDP-2 is limited, this study calculated similar accumulated olivine constraints (Mg#≤75) as a previous study on HSDP-1 samples (Mg#≤76) {*Baker et al., 1996*}. Using MELTS, modal and modeled estimates differ by less than 8.9 vol. %, giving confidence to our results.

1. INTRODUCTION

Before the Hawaii Scientific Drilling Project (HSDP) broke ground in December of 1993 near Hilo Bay, Hawaii, the continuous evolution of a single "hot-spot" volcano had not been sampled directly. Prior to this HSDP pilot hole, the history of an individual volcano was a patchwork of surface and ocean dredging samples *(Stolper et al., 1996)*. By 1999, phase 2 of the HSDP drilled into the southwestern flank of Mauna Kea (MK) at Hilo Bay to a maximum depth of 3098 meters below sea level (mbsl). The HSDP-2 core

represents the most continuous stratigraphic lava sequence of a single hotspot volcano available and includes 2853 m of MK and 245 m of overlying Mauna Loa (ML) lavas *(DePaolo et al., 2001)*. These intervals represent approximately 400 kyr and 100 kyr of eruptive history, respectively. The HSDP-2 core contains tholeiitic ML lavas, alkali/post-shield MK lavas and tholeiitic MK lavas consecutively with depth. Subaerial MK lavas extend to approximately 1078 mbsl where they transition into submarine lavas. Submarine tholeiitic MK lavas are represented by the following rock types: massive units, pillow basalts, hyaloclastites, and intrusives *(Rhodes and Vollinger, 2004)*.

Hotspot lavas are valuable because they tap into deeper mantle sources than other volcanoes. By studying the temporal geochemical evolution of these lavas, we can better understand the spatial, geochemical structure of the underlying mantle plume. The HSDP assumes that as the volcano travels across the zoned mantle plume, its source components and melt production are reflected through changes in lava compositions and eruption rates. *(Rhodes and Vollinger, 2004)*.

HSDP lavas are more olivine-rich in comparison to subaerial erupted Hawaiian shield lavas. Either the HSDP lavas have a high MgO source or they contain accumulated olivine *(Garcia, 1996)*. Hawaiian lavas represent the composition of their mantle source region only if they have not been modified by addition or removal of crystals. A previous study on the HSDP-1 samples concluded that lavas with Mg # $\geq$ 76 contain accumulated olivine *(Baker et al., 1996)*. Therefore, we suspect that the HSDP-2 lavas may also contain accumulated olivine. This study will attempt to identify the HSDP-2 samples which contain accumulated olivine. Generally speaking, if olivine crystals remain within the chamber upon eruption, then the residual liquid is increased

artificially in magnesium content. The resulting forsterite (Fo) content of the crystals would be too low to be in equilibrium with the host liquid, and thus the liquid is recognized to contain accumulated olivine. The compositions of HSDP-2 samples, which contain cumulus olivine, must be corrected so as to more accurately represent the mantle source compositions from which they come.

2. METHODS

2.1 Petrography

Forty HSDP-2 thin sections were examined using a petrographic microscope. Textural observations were noted and modal percentages of phenocrysts were quantified using the optical point counting method. Approximately 2000 point counts were taken for each thin section, covering an area of 15 x 3 mm. These modal analyses were weighted for vesicles and normalized to 100 percent. Phenocrysts were identified as "relatively large, conspicuous crystals in a porphyritic rock" (*Bates and Jackson*, 1987) and were measured to a minimum size of 0.1 mm. Strained olivine phenocrysts were not distinguished from unstrained phenocrysts in the point count in accordance with the findings of *Baker et al.* (1996), which revealed no systematic compositional variations in strained and unstrained phenocrysts for both MK and ML samples.

2.2 Geochemistry

HSDP-2 bulk chemistry data from Rhodes and Vollinger (2002) in conjunction with phenocryst modal abundance quantified in this study were used to construct an olivine control line as well as depth profiles. All depth profiles were fitted with a moving average regression line set at two periods. This regression takes a moving average between the x-values in each profile with increasing depth. Post-shield lavas, which did

not follow an olivine control line, were excluded from Figure 1. Olivine compositional data was analyzed in selected samples using the Cameca SX50 electron microprobe (beam conditions: 15keV, 30nA, 20sec, 1μm beam size) at the University of Tennessee to determine the highest Fo-content of olivine in each sample. Analyzed crystals were chosen semi-randomly and analyzed from rim to core. Compositional data in addition to bulk Mg# were used to create Figure 2. An 'equilibrium zone' was created for the samples in Figure 2 using a K_D of 0.3±0.03 *(Baker et al. 1996).* The magma chamber modeling program, MELTS (*Ghiorso and Sack*, 1995), was used along with bulk chemistry to predict both olivine abundance and maximum Fo-content of the olivine phenocrysts within the select samples analyzed for compositional data. All iron was input into MELTS as Fe_2O_3 and the ratios of FeO to Fe_2O_3 for each sample were calculated. In order to determine the liquidus temperature for each sample, the *f*O2 was set at the QFM buffer and ran at 1 atm pressure. The simulated magma composition of each sample was cooled from the liquidus temperature down to ~800°C in increments of 10°C. Information regarding the liquidus temperature, maximum Fo-content of olivine, and modal abundance of olivine was recorded in Table 2 and used to decide which samples contained accumulated olivine. Predicted modal abundances from the MELTS program were compared to the measured modal abundances of this study to assess confidence in our modal estimations.

3. RESULTS

3.1 Petrography

In general HSDP-2 samples are hypidiomorphic-granular and vary in crystallinity from holocrystalline to vitrophyric (Plate 1). Vesicularity ranges from 0-24.4 vol% and

is not depth dependent. Most samples are porphyritic and contain phenocrysts of olivine, clinopyroxene, and/or plagioclase. Quench and flow textures occur in a minimal number of samples (Plate 2). Glomerocrysts are displayed in select samples and do not correlate with depth (Plate 3). Olivine phenocrysts range in size from 0.4-4.6 mm and display concentric zoning, resorption features, simple twins, and melt inclusions throughout the HSDP-2 core (Plate 4). A maximum of 57.1% of olivine phenocrysts within a single sample alter to serpentine and/or iddingsite (Plate 5). Strained olivine phenocrysts with kink-banded extinction were observed in most samples (Plate 6). Plagioclase phenocrysts range from 0.2-2.9 mm and readily alter to sericite in many samples. They show albite twinning and subophitic texture (Plate 3). Radiating laths of skeletal plagioclase can be seen in sample SR967 and attest to the presence of quench textures in HSDP-2 samples. Phenocryst abundances range from 5.3-50.3 vol% for olivine, 0-18.9 vol% for plagioclase, and 0-4.1 vol% for clinopyroxene (Table 1). Thus the samples range from aphyric to highly olivine-phyric basalts. Modal percentages of olivine do not vary systematically with depth for ML or MK samples.

3.2 Geochemistry

When compared to bulk MgO, olivine phenocryst abundance defines an olivine control line with an R^2 value = 0.85 (Figure 1). As seen in Figure 2, the compositional ranges of olivine for samples SR741, SR531, SR490, and SR574 do not intersect the K_D 'equilibrium zone.' All of these samples have a MELTS modeled Fo-content higher than the measured Fo-content and correspond to a Mg# $\geq$75, with the exception of SR741 (Table 2). The maximum difference between the MELTS modeled and measured olivine vol % is <8.9%. MELTS modeled FeO and measured FeO differ at most by 1.1 wt.%.

Compositional ranges of Fo_{88-90} within the MK tholeiitic lavas correspond to a wide range of modal olivine (13.5-30.1vol%) (Table 2). The depth profiles of olivine vol %, Ni ppm, and Cr ppm, mimic each other (Figure 3). Liquidus temperatures range from 1423-1497°C and represent the onset of spinel crystallization. Olivine crystallization began an average of 92.4°C after spinel crystallization (Table 2). The depth profiles of olivine vol% and Mg# resemble one another (Figure 4). Using olivine accumulation criteria from Figure 3, nine HSDP-2 samples of variable depth are highlighted as suspect in Figure 5. Figure 6 shows those samples for which olivine accumulation was confirmed using both compositional and bulk data.

4. DISCUSSION

4.1 Petrography

HSDP-2 samples display a wide range of textures. Crystals within each sample vary in size, shape, abundance, and degree of alteration. With a modal range of 5.3-50.3 vol%, olivine phenocrysts are the most abundant phenocrysts in HSDP-2 samples overall. Resorption textures within olivine phenocrysts are physical indications of disequilibrium. Because these textures are present in samples other than those which follow the selection criteria for olivine accumulation, it can be said that other samples may be in disequilibrium. Thus these samples may need to be corrected for alternative compositional inconsistencies so as to represent mantle source compositions. Phenocryst size ranges and textural descriptions of HSDP-2 samples concur with studies by *Garcia (1996)* and *Baker et al. (1996).*

4.2 Geochemistry

Because MgO and olivine abundance follow an olivine control line it can be said that the bulk chemistry of HSDP-2 lavas is governed by olivine abundance. Samples with measured Fo-content less than modeled Fo-content (Table 2) and with Mg# ≥75 which do not intersect the KD 'equilibrium zone' (Figure 2) contain accumulated olivine. Cumulus olivine artificially increases the magnesium content of residual liquids within the magma chamber. For this reason, olivine accumulation will be a probable cause of misrepresentation of HSDP-2 mantle source compositions. Although the compositional data set for HSDP-2 is limited, this study calculated similar accumulated olivine constraints (Mg#≥75) as a previous study on HSDP-1 samples (Mg#≥76) *(Baker et al. 1996)*. As noted in previous sections, sample SR741 follows one of the selection criteria for cumulus olivine. However, because SR741 is surrounded by two other samples (SR603 and SR967) which intersect the K_D 'equilibrium zone' and do not contain accumulated olivine, it is likely that we failed to measure the most forsteritic olivine in this sample (Figure 2). The closeness of fit between measured and modeled FeO and olivine modal abundance adds confidence to our modal estimates. Olivine is the primary host phase of Ni during crystallization; thus, the positive correlation between Ni ppm and olivine abundance with depth further supports our modal estimates (Figure 3). Interestingly enough, Cr ppm also shows a positive correlation with olivine abundance with depth (Figure 3). Because chromium is concentrated in a spinel, the positive correlation observed between the corresponding depth profiles may suggest co-crystallization and co-accumulation of spinel and olivine. Seeing that the MELTS calculated temperatures at which spinel and olivine begin to crystallize vary by less than

100°C, and that the crystallization of both minerals overlaps for the majority of their cooling history, co-crystallization is probable for HSDP-2 samples. The resemblance between the depth profiles of olivine abundance and Mg# (Figure 5) further supports the claim that HSDP-2 samples follow an olivine control line. The samples highlighted for olivine accumulation in Figure 6 show no systematic variation with depth. This profile shows a slight cyclical pattern most likely related to olivine accumulation and subsequent magma recharge. This pattern might be better seen with the addition of more data points.

5. SUMMARY

HSDP-2 samples display a wide range of textures. Crystals within each sample vary in size, shape, abundance, and degree of alteration. HSDP-2 samples with Mg#≥75 and measured Fo-content less than the modeled Fo-content, and which do not intersect the K_D 'equilibrium zone', contain accumulated olivine. Therefore, not all HSDP-2 lavas represent mantle compositions. Select samples must be corrected for accumulated olivine. Samples with a Mg#<75 whose olivine composition falls below the equilibrium Fo range probably reflect the lack of measuring the most Fo-rich phenocryst. Limited data sets for HSDP-2 samples yielded similar olivine accumulation constraints as previous studies (*Baker et al., 1996*). Confidence in estimated modal abundances for HSDP-2 samples is strengthened by the low variability between measured and MELTS modeled estimates and the positive correlation of Ni ppm and olivine (vol%) with depth. In closing, samples which contain accumulated olivine have been identified using the aforementioned selection criteria. Without corrections for olivine accumulation, these samples cannot accurately resemble their parent magma source.

REFERENCES

Baker, M.B., S. Alves, and E. M. Stolper, Petrography and petrology of the Hawaii Scientific Drilling Project lavas: Inferences from olivine phenocryst abundances and composition, *Journal of Geophysical Research*, 101, B5, 11,715-11,727,1996.

Bates, R.L. and J.A. Jackson, *Glossary of Geology*, 788 pp., American Geological Institution, Alexandria, V.,1987.

DePaolo, D.J., E. Stolper, and D.M. Thomas, Deep Drilling into a Hawaiian Volcano, *EOS*, 82, 13, 149-160, 2001.

Garcia, Michael, Petrography and olivine and glass chemistry of lavas from the Hawaii Scientific Drilling Project, *Journal of Geophysical Research*, 101, B5,11,701-11,713, 1996.

Ghiorso, M. S. and R.O. Sack, Chemical mass transfer in magmatic processes, IV, A revised and internally consistent thermodynamic model for the interpolation and extrapolation of liquid-solid equilibria in magmatic systems at elevated temperatures and pressures, *Contributions to Mineralogy and Petrology*, 119, 197-212, 1995.

Rhodes, J.M. and M.J. Vollinger, Composition of Basaltic Lavas by Phase-2 of the Hawaiian Scientific Drilling Project: Geochemical Stratigraphy and Magma Types, *Geochemistry, Geophysics, Geosystems*, 5, 2004.

Stolper, E.M., D. DePaolo, and D. Thomas, Introduction to special section: Hawaii Scientific Drilling Project, *Journal of Geophysical Research,*101, 11,593-11,597, 1996.

Appendix

Table 1: Phenocryst Modal Abundances

Sample	Unit	Depth (m)	MgO (wt%)	Ol (vol%)	Plag (vol%)	Cpx (vol %)
SR0008-2.70	2	-9.5	7.64	6.5	2.5	2.7
SR0036-1.22	8	-53.4	24.24	50.2	0	0
SR0129-5.20	47	-267.5	6.93	5.3	12.2	1.7
SR0133-8.20	49	-281.4	15.63	28.0	3.4	1.2
SR0141-7.90	56	-305.8	7.14	6.2	0	1.9
SR0193-0.00	80	-443.7	10.86	13.5	0	4.1
SR0240-3.30	98	-563.6	16.77	22.2	0	0
SR0256-0.95	103	-589.2	7.97	8.9	0	3
SR0276-7.85	110	-636	21.57	41.7	0	0
SR0300-6.50	119	-695.9	14.08	18.1	0	1.4
SR0340-1.00	132	-793.7	24.76	38.0	0	1.8
SR03454-7.75	138	-834	22.31	39.3	0	0.2
SR0372-2.80	142	-871.2	8.17	8.4	0.1	0.5
SR0472-1.00	185	-1123.2	8.44	11.9	7.2	1.2
SR0490-1.50	190	-1229.7	17.96	28.6	0.00	0
SR0531-4.40	198	-1352.6	17.88	31.0	0.00	0.8
SR0545-8.35	198	-1395	18.26	40.0	0.00	1.3
SR0574-1.90	202	-1474.8	18.56	39.2	0.2	2.4
SR0603-8.90	216	-1548.2	13.01	20.9	0.00	1.2
SR0664-5.10	238	-1705.6	15.90	**28.3**	0.3	0.2
SR0694-9.00	253	-1794.9	11.22	21.9	1.4	1.1
SR0723-13.70	270	-1933.9	7.96	7.1	4	0.4
SR0732-1.10	274	-1973.9	9.9	18.5	0	1.5
SR0741-7.90	278	-2009.8	16.21	30.1	0.7	0.7
SR0768-11.20	285	-2157.5	6.76	8.1	13.7	0.7
SR0776-17.70	286	-2209.6	7.85	6.6	2.5	0.5
SR0850-5.95	305	-2551	6.44	7.9	11.8	1.2
SR0860-8.10	310e	-2615	7.77	20.2	20	2.7
SR0871-13.00	312	-2654.3	16.64	26.5	0.00	2.9
SR0916-1.15	330	-2837.7	16.53	30.7	0.00	0.4
SR0939-18.10	335a	-2961.2	17.5	31.3	0.3	3.8
SR0956-18.35	343a	-3019.2	7.01	13.4	8.2	0.7
SR0967-2.75	341b	-3069	15.39	30.1	14.8	1.4

Sample #	Liquidus Temperature (°C)	Olivine Crystallization Begins (°C)	measured olivine (vol%)	modeled olivine (vol%)*	measured Fo content	modeled Fo content	Bulk Mg#	Accumulated Olivine
sr490	1497	1397	28	26.7	88.29	90.17	76	yes
sr531	1491	1411	31	31.32	89.22	90.58	75	yes
sr574	1493	1423	39	30.09	90.19	90.92	77	yes
sr603	1423	1302	21	13.49	89.52	86.95	70	no
sr741	1471	1380	30	26.2	87.62	89.64	73	no
sr967	-	1369	30	21.39	89.78	89.28	74	no

Table 2: MELTS data, modal abundance data and Bulk chemistry (Mg#)

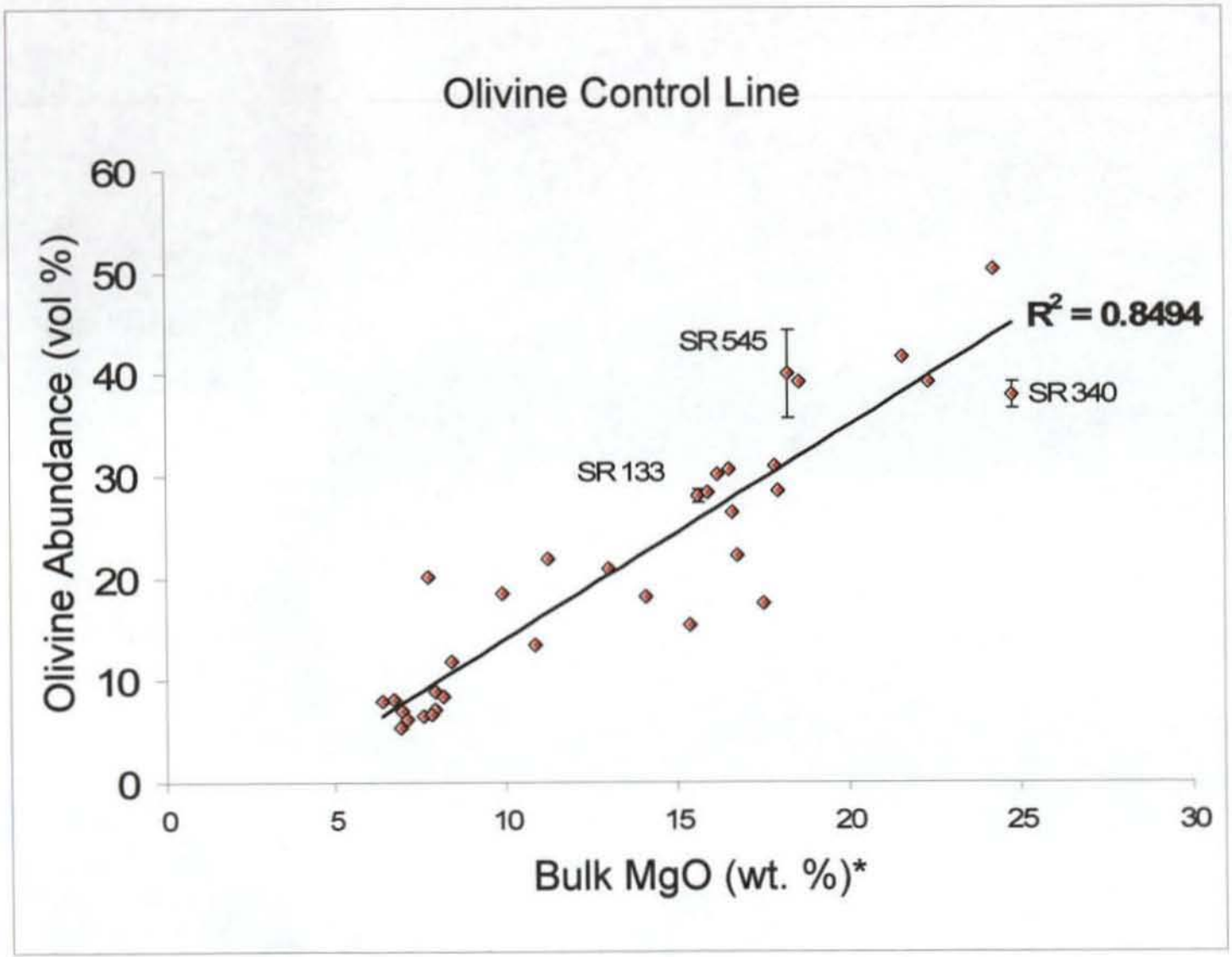

Figure 1: Olivine control line with error bars for olivine modal abundance included; post shield MK lava SR 121 and main shield MK SR431 excluded from figure

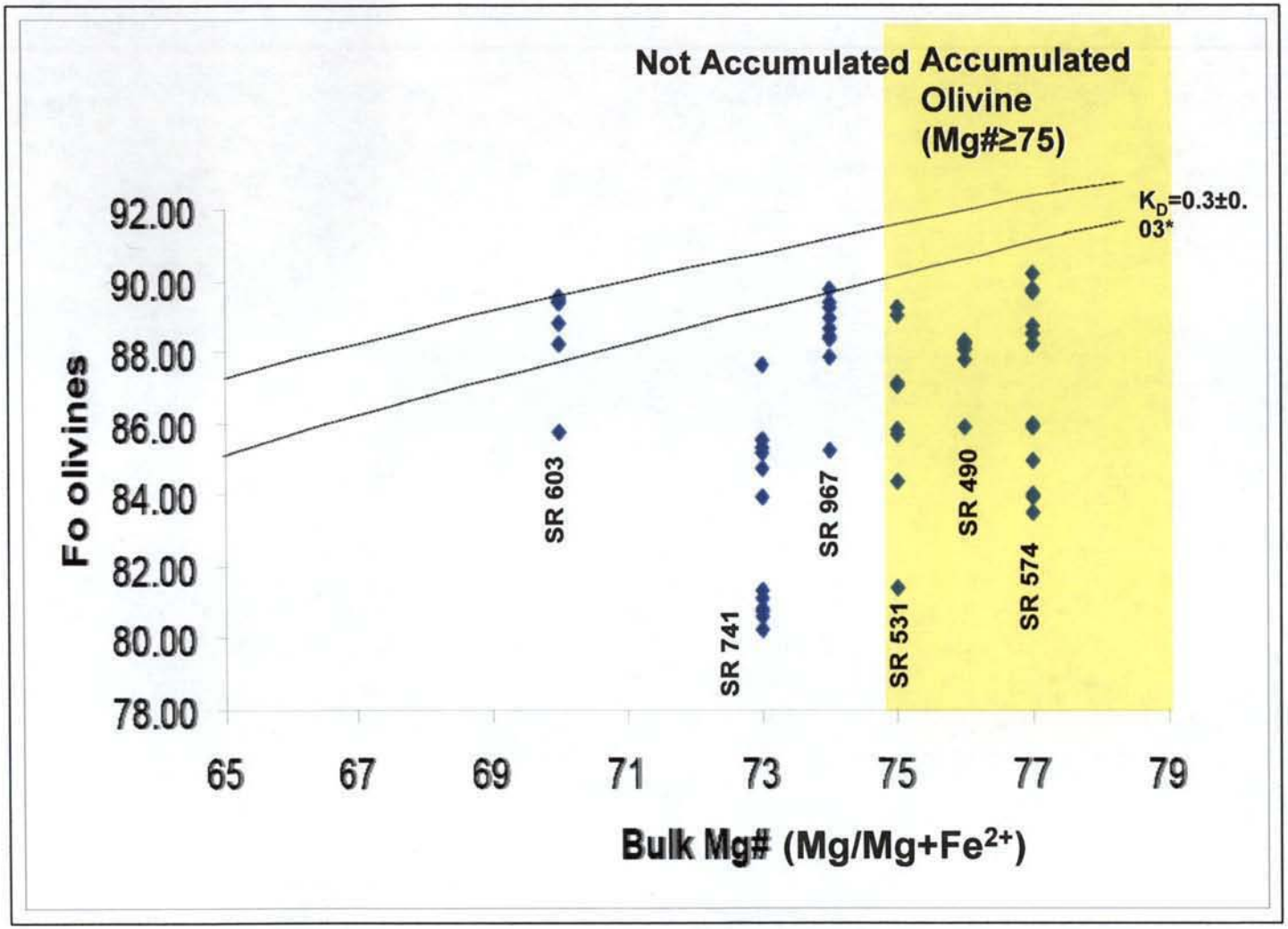

Figure 2: Bulk Mg # vs. measured Fo range within select samples. Parallel lines represent equilibrium olivine-liquid conditions {lines using a KD= 0.3±0.03.5 Yellow box represents samples with accumulated olivine.

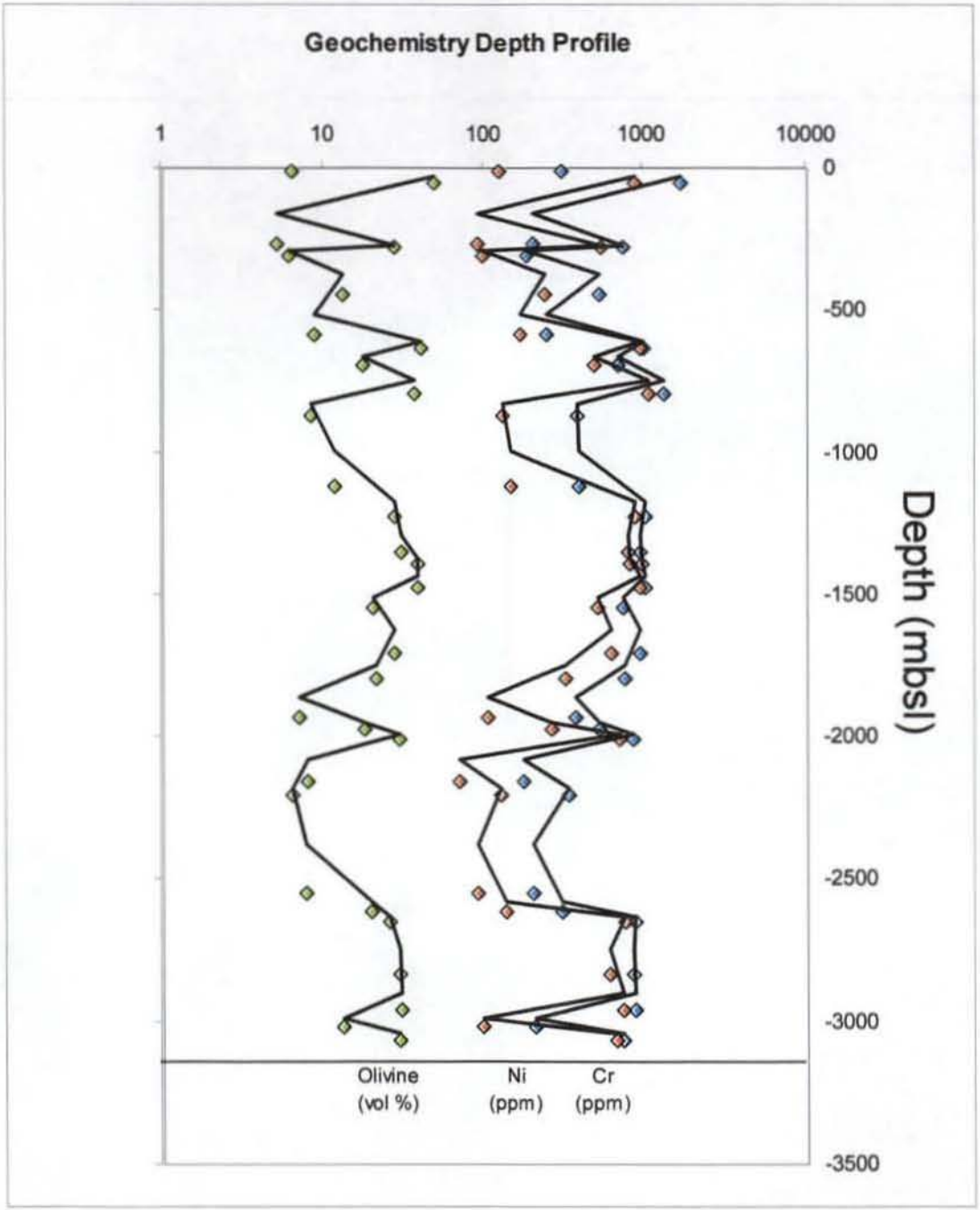

Figure 3: Depth profiles of Olivine Phenocryst Abudance, bulk rock Ni and Cr {moving average trend line; period 2}

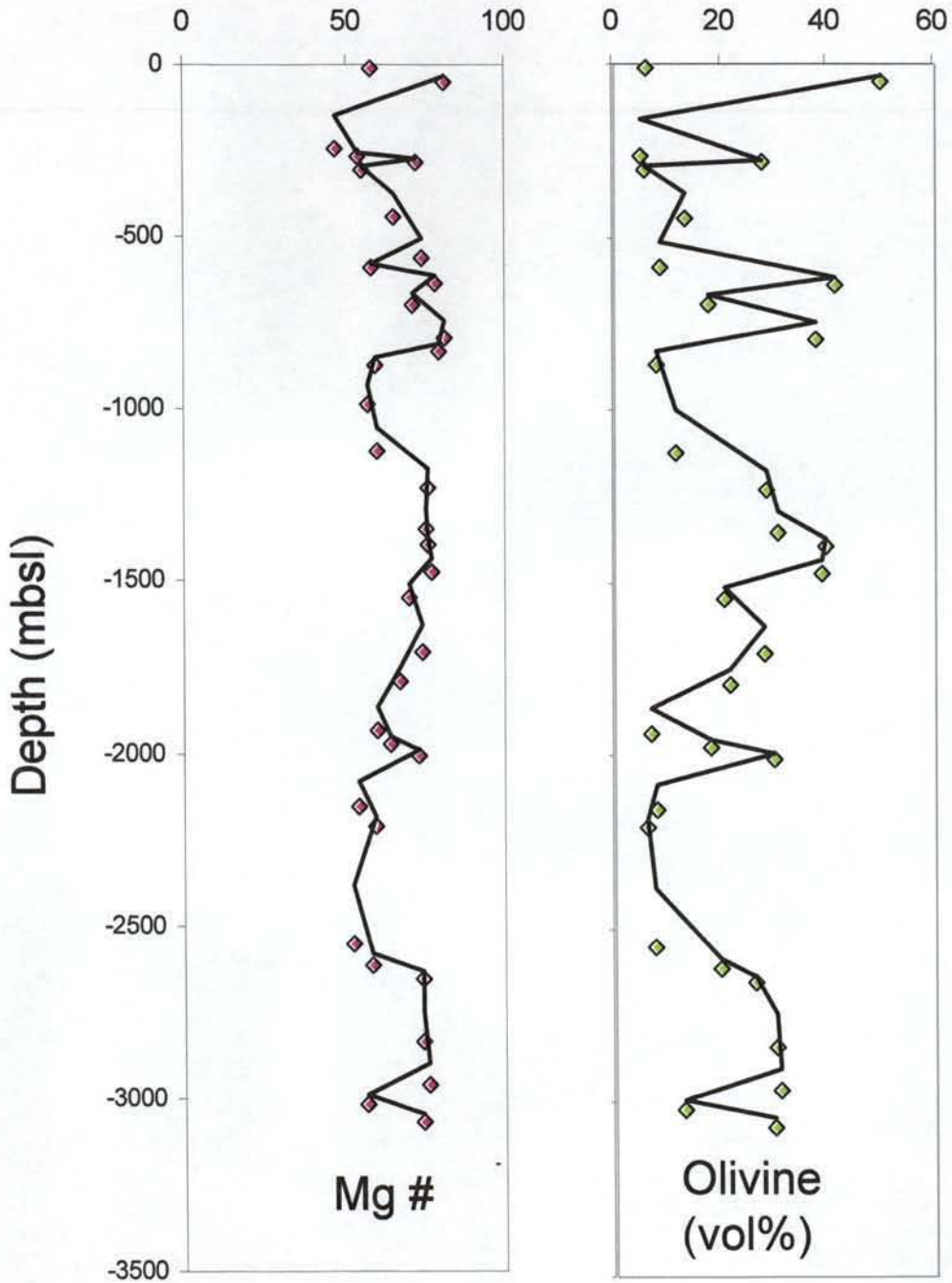

Figure 4: Depth Profile of Mg# and Olivine Modal Abundance {moving average trend line; period 2}

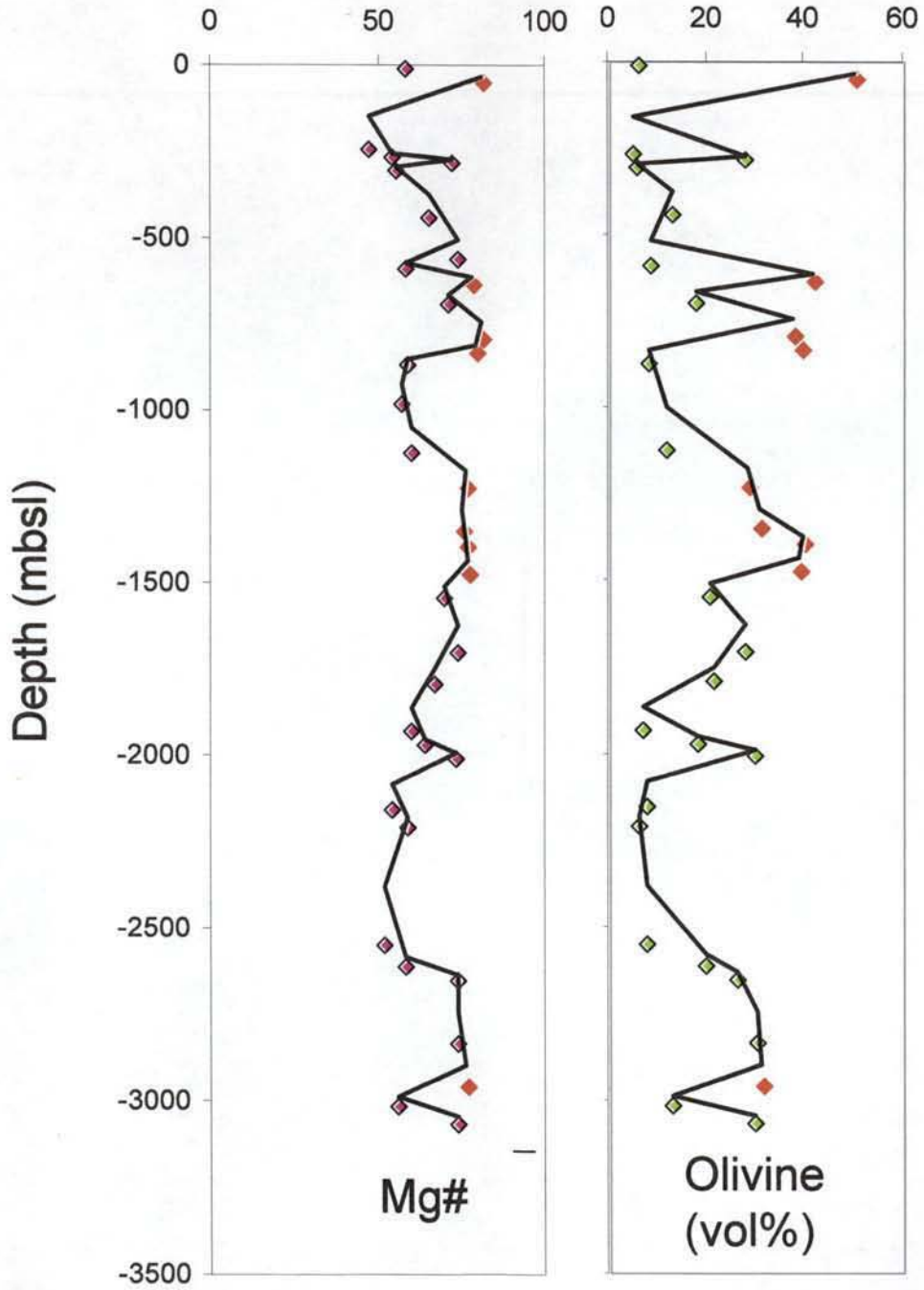

Figure 5: Depth profile of suspected samples for olivine accumulation {moving average trend line; period 2}

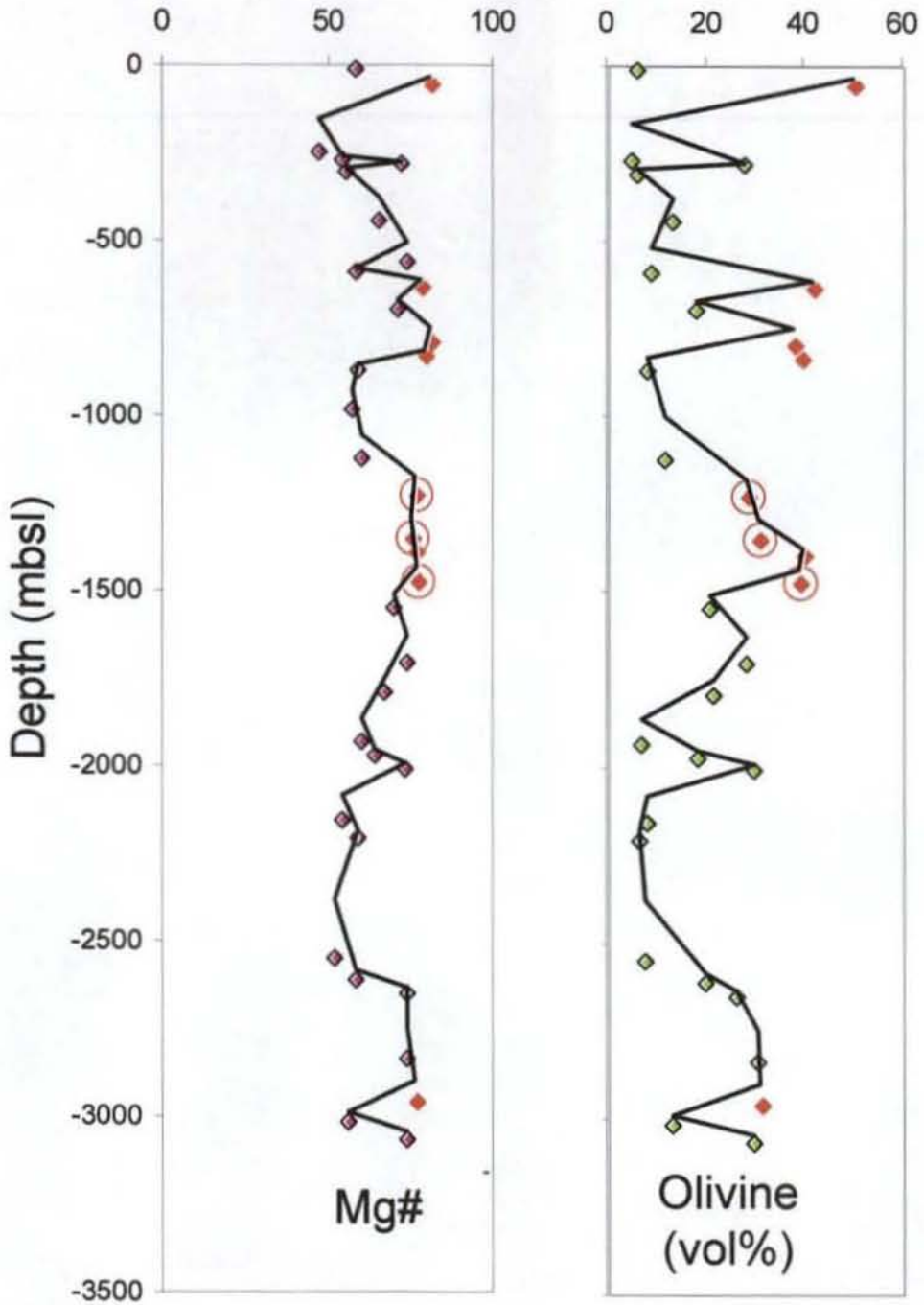

Figure 6: Depth Profile of samples with accumulated olivine and with Mg≥75 {moving average trend line; period 2}

Accumulated Olivine (Fo modeled>Fo measured and Mg≥75

Mg≥75

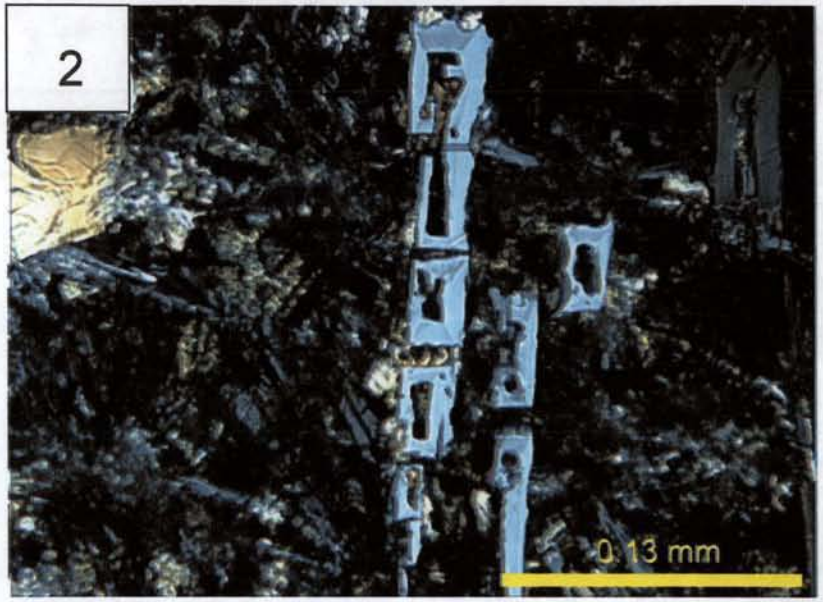

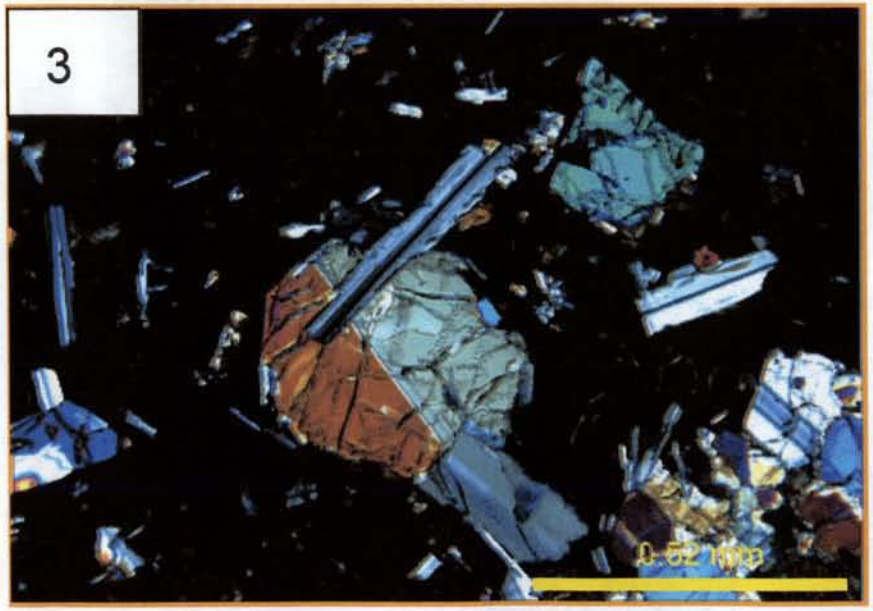

Plate 1: Vitrophric texture with plagioclase mirolites

Plate 2: Skeletal plagioclase quench texture

Plate 3: Glomercryst with subophitic plagioclase

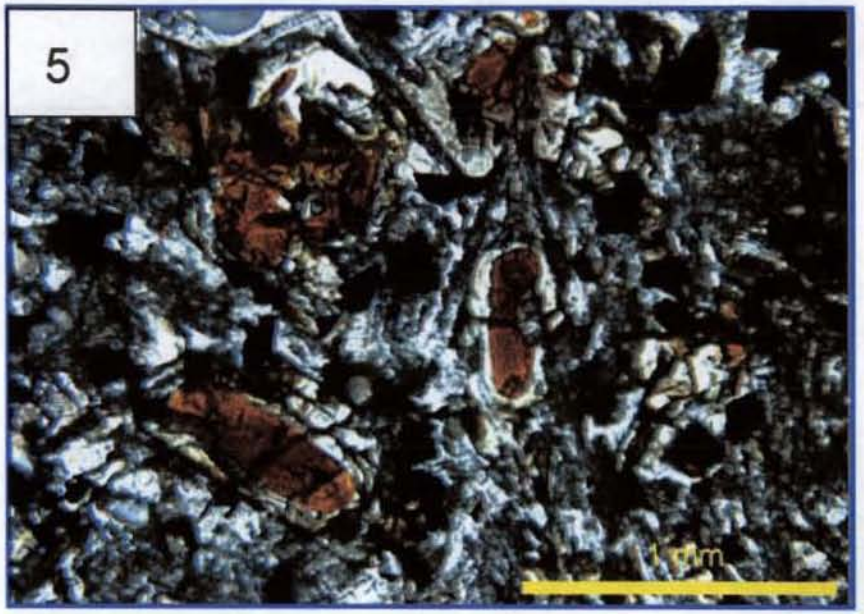

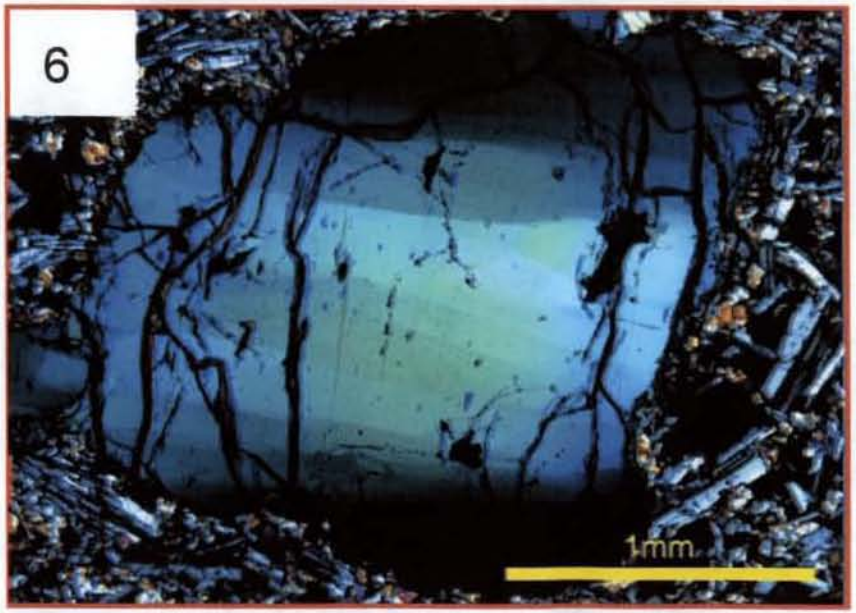

Plate 4: Olivine resorpition texture along concentric zoning

Plate 5: Alteration of olivine cores to iddingsite

Plate 6: Strained olivine phenocryst

0.51 mm

SR121: Plagioclase Phenocryst with sericite alteration

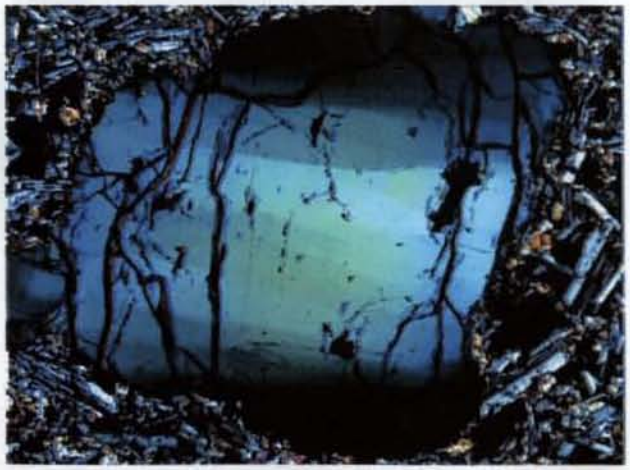

0.51 mm

SR36: Strained Olivine Phenocryst

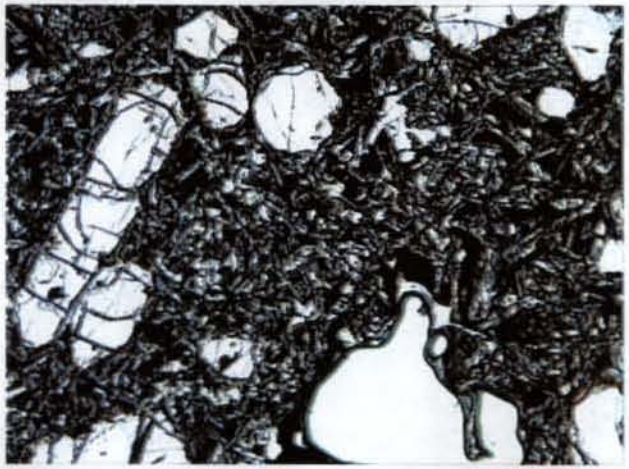

0.51 mm

SR117: Elongate and Equant Olivine Phenocrysts in plane polarized light

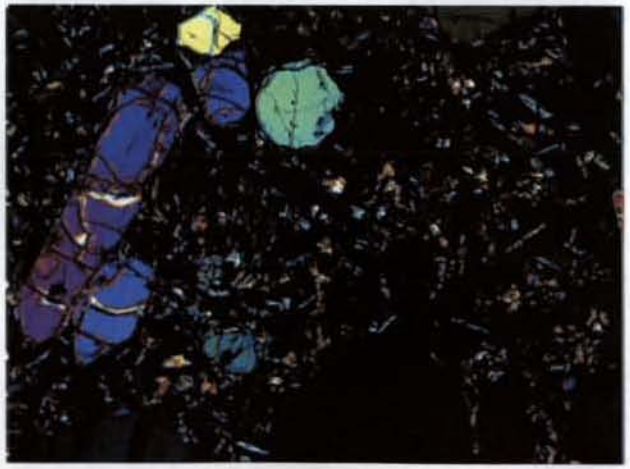

0.51 mm

SR117: Elongate and Equant Olivine Phenocrysts in crossed polarized light

0.13 mm

SR121: Olivine Core Altered to Iddingsite

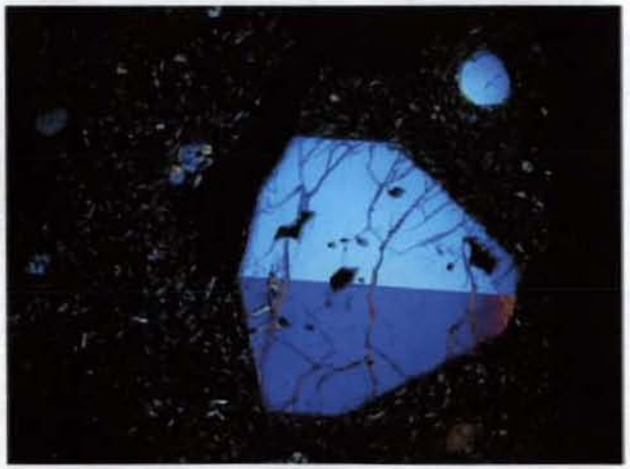

1.29 mm

SR193: Twinned Olivine Phenocryst

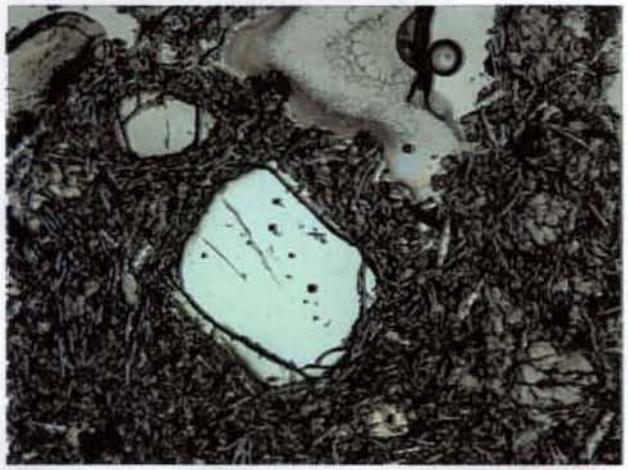

0.51 mm

SR276: Olivine phenocryst (center) vesicle (top)

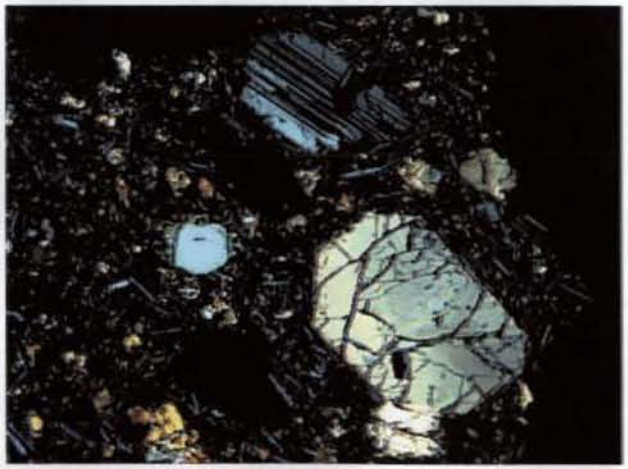

0.51 mm

SR276: Plagioclase phenocryst albite twinning

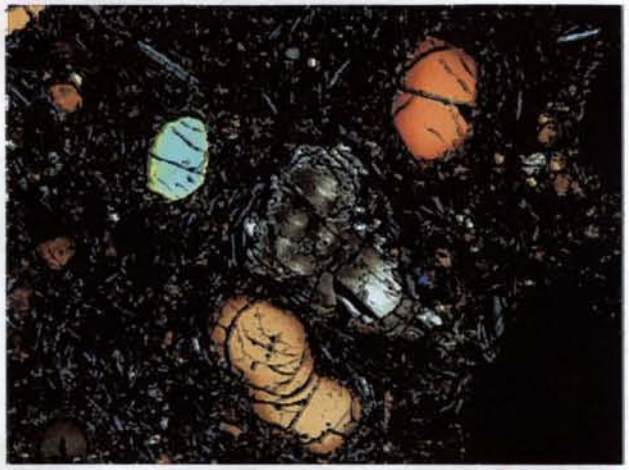

0.51 mm

SR276: Olivine Phenocrysts and Sericitization of Plagioclase

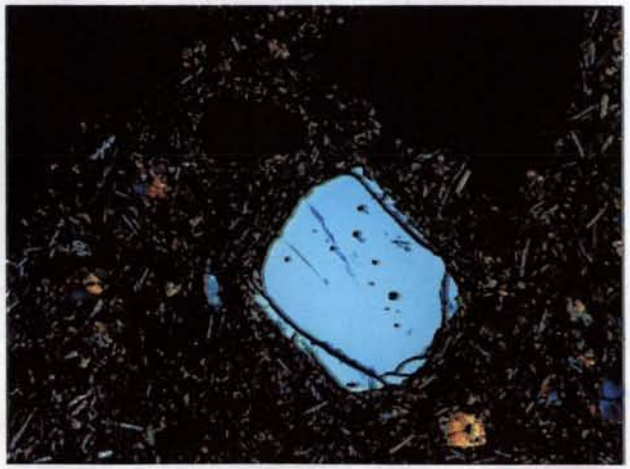

0.51 mm

SR276: Olivine phenocryst in plane polarized light

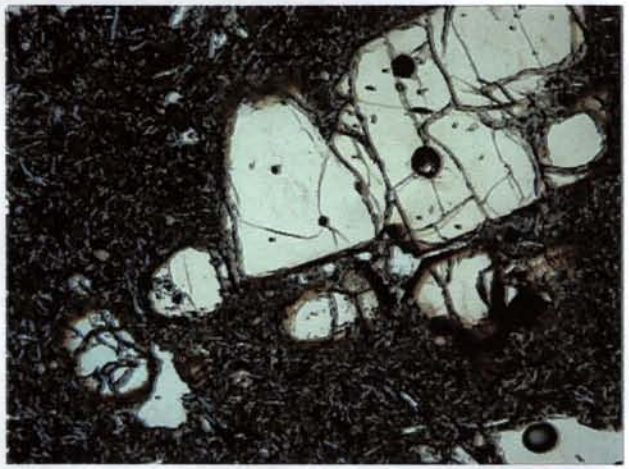

0.51 mm

SR300: Fractured Olivine Phenocryst with Iddingsite alteration rim

0.13 mm

SR354: Strained Olivine with kink-banding. Iddingsite alteration along the bands.

0.51 mm

SR354: Strained Olivine Phenocrysts with Iddingsite Alteration in crossed polarized light.

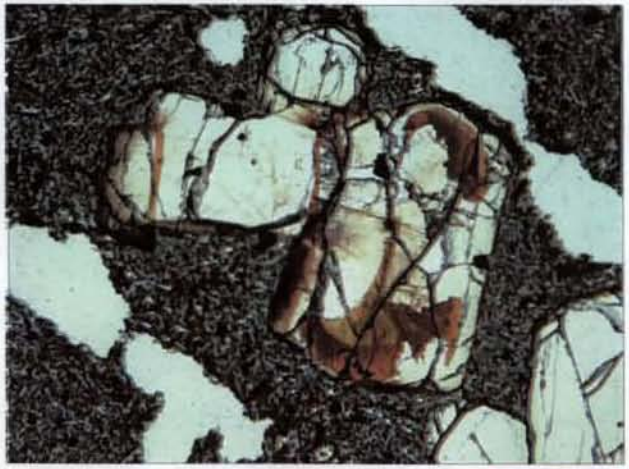

0.51 mm

SR354: Strained Olivine Phenocrysts with Iddingsite Alteration in plane polarized light.

1.29 mm

SR413: Xenolith within sample; notice finer grained oval-shaped section (center)

0.26 mm

SR413: Photo of textural differences between xenolith (left) and groundmass (right)

? mm

SR472: Olivine Phenocryst with concentric zoning and resorption

1.29 mm

SR655: Olivine cluster and bimodal distribution of olivine phenocrysts

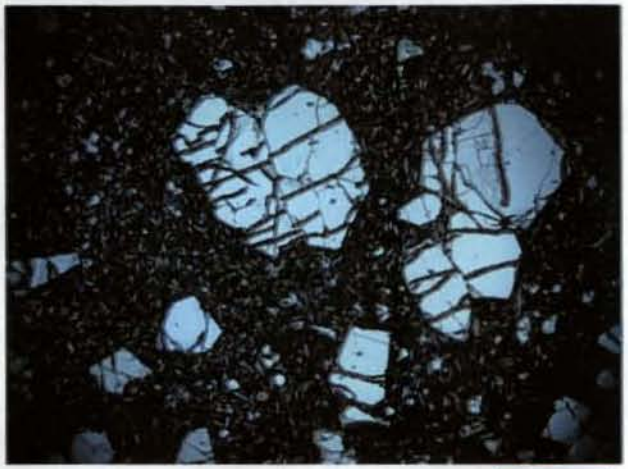

1.29 mm

SR545: Olivine Phenocrysts in plane polarized light with serpentine alteration

1.29 mm

SR545: Olivine Phenocrysts in crossed polarized light with serpentine alteration

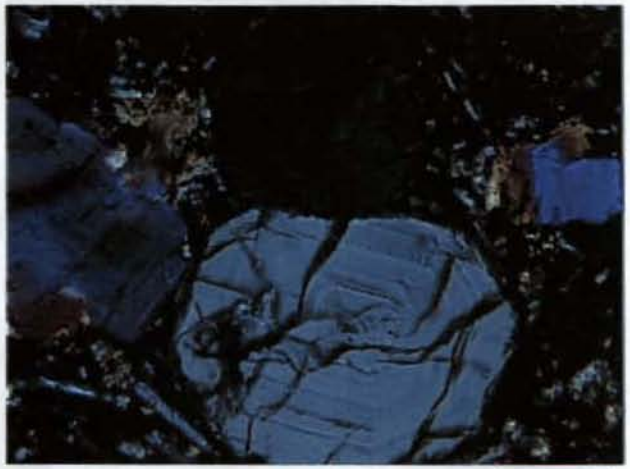

0.07 mm

SR603: Concentric Zoned Olivine Phenocrysts in crossed polarized light

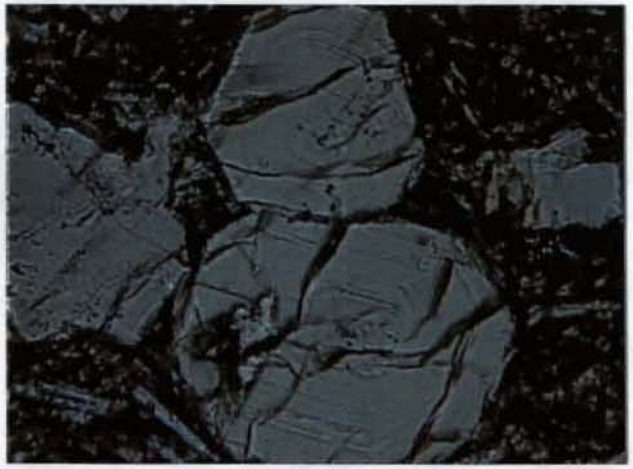

0.07 mm

SR603: Concentric Zoned Olivine Phenocrysts in plane polarized light

0.51 mm

SR655: Olivine phenocryst showing resorption

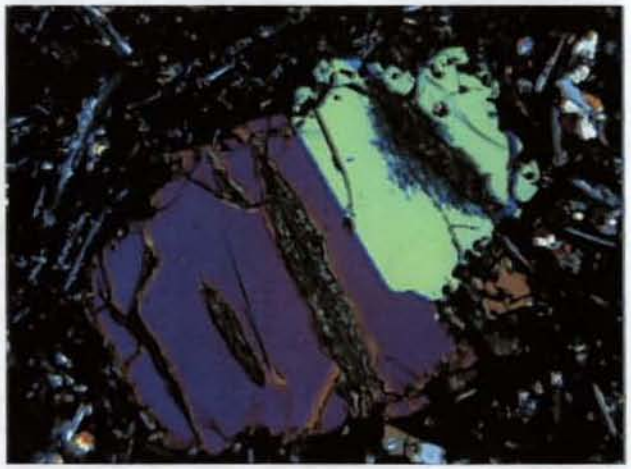

0.26 mm

SR655: Olivine phenocryst showing resorption at edges

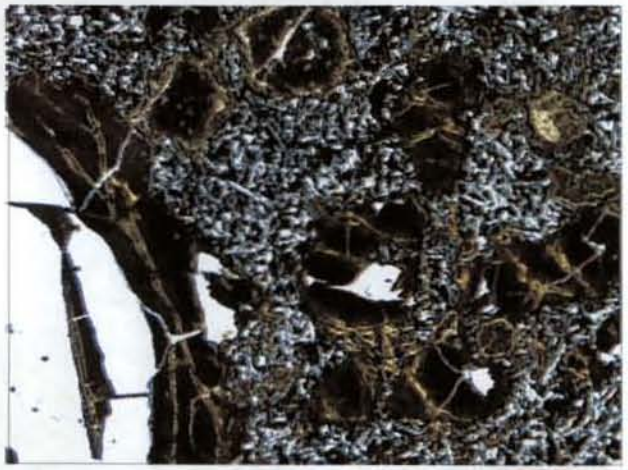

0.51 mm

SR664: General alteration

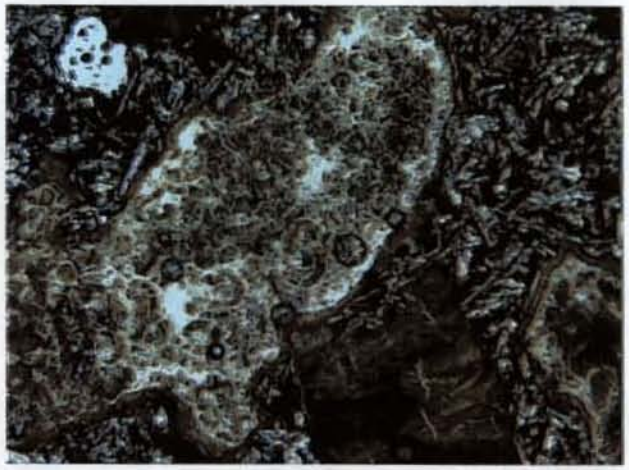

0.26 mm

SR664: Alteration and formation of amygdule

0.26 mm

SR694: Strained elongate olivine phenocryst with resorption

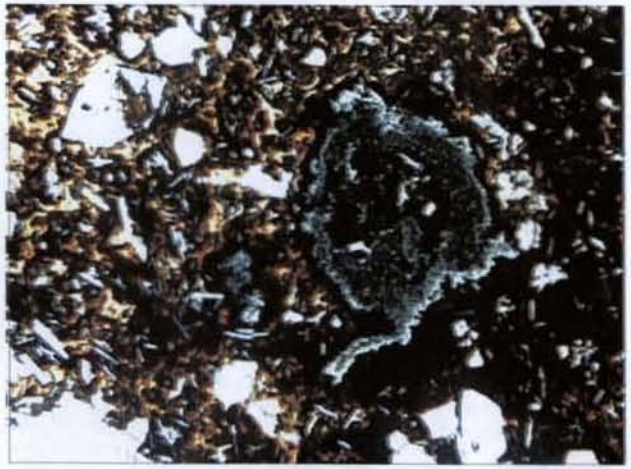

0.51 mm

SR723: Glassy groundmass and amygdaloidal texture

0.51 mm

SR723: Glomerocryst of olivine and plagioclase laths

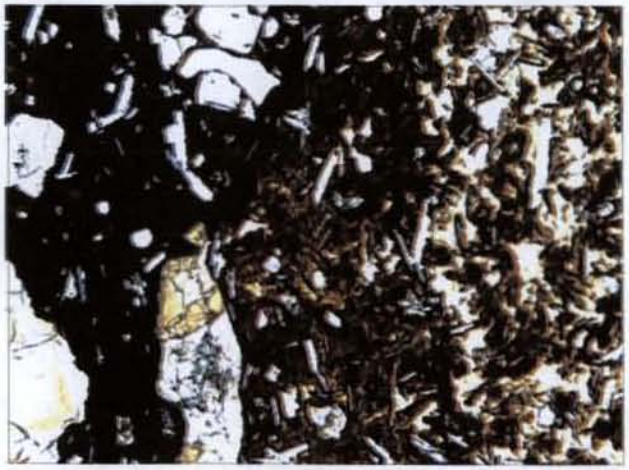

0.51 mm

SR723: Two different colors of glass in groundmass; microlites present

0.13 mm

SR732: Olivine phenocrysts with melt inclusions in plane polarized light

0.13 mm

SR732: Olivine phenocrysts with melt inclusions in cross polarized light

0.26 mm

SR776: Zoned Equant Olivine Phenocryst

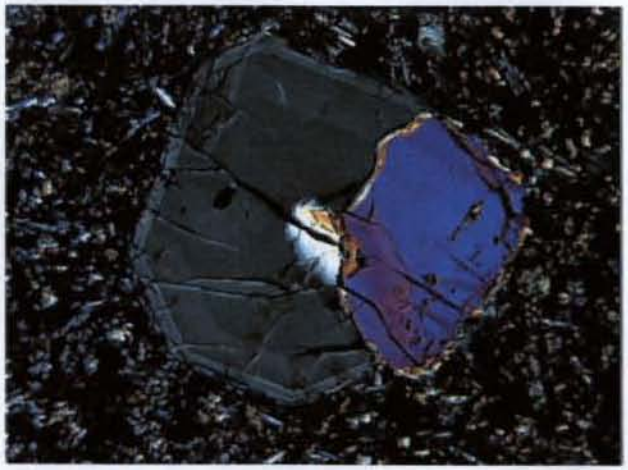

0.13 mm

SR776: Zoned Equant Olivine Phenocryst

0.51 mm

SR967: Radiating Plagiocase Laths

0.13 mm

SR967: Radiating Plagioclase Laths and Skeletal Plagioclase.

Photo Gallery of Hawaiian Basalts: A Textural Guide

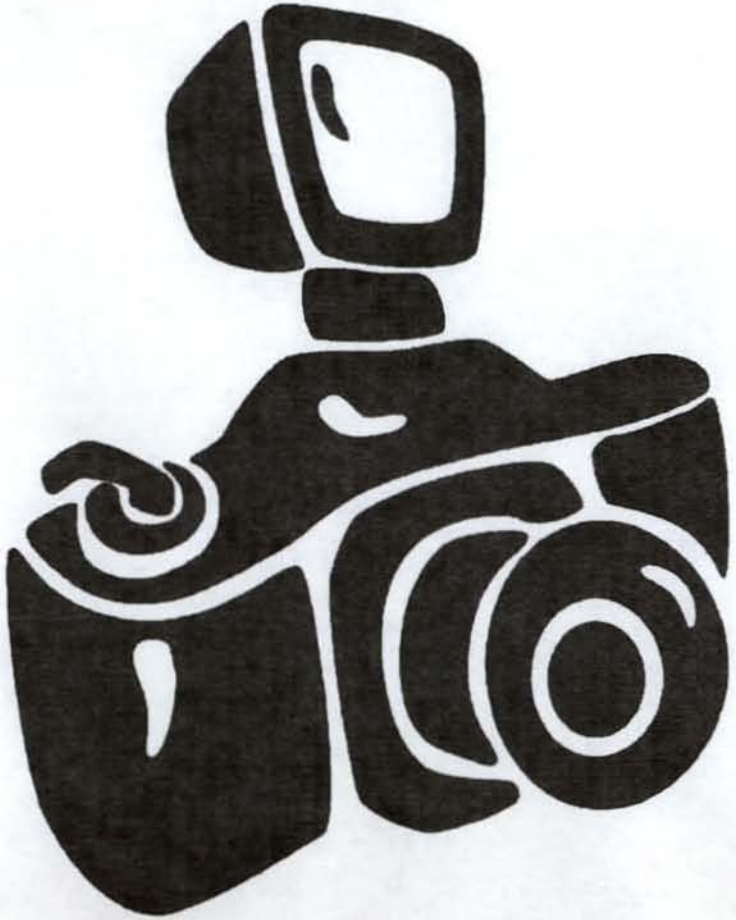

Shelley D. Miller

Senior Thesis Project Appendix (Spring 2005)